Reprint from Proceedings of the 19th International Conference on Pattern Recognition (ICPR), Tampa, FL, 2008

Quantitative abdominal fat estimation using MRI

O. Dahlqvist Leinhard[1,3], A. Johansson[1,2], J. Rydell[2,3], Ö. Smedby[1,3], F. Nyström[1], P. Lundberg[1,3], and M. Borga[2,3]
[1]Department of Medical and Health Sciences, [2]Department of Biomedical Engineering, [3]Center for Medical Image Science and Visualization (CMIV), Linköping University, Sweden.
Corresponding author: Olof Dahlqvist Leinhard, email: oloda@imv.liu.se

Abstract

This paper introduces a new method for automatic quantification of subcutaneous, visceral and non-visceral internal fat from MR-images acquired using the two point Dixon technique in the abdominal region. The method includes (1) a three dimensional phase unwrapping to provide water and fat images, (2) an image intensity inhomogeneity correction, and (3) a morphon based registration and segmentation of the tissue. This is followed by an integration of the corrected fat images within the different fat compartments that avoids the partial volume effects associated with traditional fat segmentation methods. The method was tested on 18 subjects before and after a period of fast-food hyper-alimentation showing high stability and performance in all analysis steps.

1. Introduction

Obesity is today a growing problem in many parts of the world. According to [1], more than 50 % of the adults in the US suffered from abdominal obesity during 2003–2004. It is generally considered that the unfavorable prognosis in sedentary subjects with abdominal obesity is due to large amounts of intra-abdominal fat [2]. In order to study such effects, we have developed a novel method for quantitatively measuring the abdominal fat composition from MR images. The method measures three different types of fat: subcutaneous, visceral and non-visceral internal.

In order to avoid operator dependence and extensive manual work the method is fully automated. This distinguishes it from most previously published methods. Furthermore, the method should be able to quantitatively measure the fat content in each individual voxel in order to avoid partial volume effects. The proposed method consists of a number of different steps: Phase correction of two point Dixon images, intensity inhomogeneity correction and segmentation of the different types of fat.

2. Materials and methods

2.1. Subjects and data acquisition

18 healthy subjects (12 males and 6 females) were examined before and after a period of fast food based hyper-alimentation [9] using a 1.5 Tesla Achieva MR-scanner (Philips Medical Systems, Best, The Netherlands). A four element body coil was used to obtain magnitude and phase images from two different stacks using a field of view of 290 x 410 x 200 mm^3, 5 mm slice thickness and 2.14 x 2.16 mm^2 in-plane resolution, covering the abdominal region from the diaphragm to the bottom of the pelvis. A dual echo, multi slice, spoiled, fast gradient echo pulse sequence was used. The first echo was obtained using TE_1 = 2.3 ms with the water and fat signals 180° out of phase, and the second using TE_2 = 4.6 ms with the signals in phase. The repetition time was 286 ms and the flip angle was 80°. Data was collected using breath hold technique and CLEAR reconstruction.

2.2. Two point Dixon imaging

Fat content can be measured using MRI in several different ways. Since the T1 relaxation time of adipose tissue is shorter than that of most other types of tissue, segmentation of T1 weighted images are commonly used. However, due to partial volume effects, this technique has been shown to consistently underestimate the fat volume [4].

Here we have used so called Dixon imaging [5] which provides two images: one showing the fat content in each voxel and one showing the water content in each voxel. Hence Dixon images are not adversely affected by partial volume effects. As explained in section 3, separate water and fat images are also useful in the segmentation process. Because of these significant advantages, the method was based on Dixon images.

In short, Dixon imaging is performed by acquiring two separate images: one where the signals from fat and water are 180° out of phase ($I_1 = w - f$) and one where they are in phase ($I_2 = w + f$). Ideally, water and fat can then be obtained as the sum and difference of these images, respectively, and the total fat content in any region of interest can then easily be calculated. However, in practice, magnetic field inhomogeneities cause the complex phase of I_1 and I_2 to vary over the images and a robust phase correction is needed before w and f can be calculated. Several different methods for correcting Dixon images have been proposed in i.e. [6, 7, 8]. We have applied the method introduced in [3, 12], which has been shown to perform well even in the presence of severe phase artefacts.

2.3. Intensity inhomogeneity correction

In MRI the inhomogeneous sensitivity of the RF-coils cause variations in the image magnitude over the field of view. The variation in sensitivity affects the signal strength within the 3D volume and furthermore it makes comparison of signal intensities between different examinations difficult. This nonuniformity degrades the quality of the fat content estimation, and therefore needs to be eliminated.

The correction method applied here was based on two assumptions: that the intensity non-uniformity varied gradually across the image, and that it was approximately the same in the fat image f and in the in phase image I_2. The latter is important since it implies that the relative fat content $f_r = f/I_2$ is insensitive to intensity variations.

Voxels containing pure adipose tissue can easily be identified by a simple thresholding of f_r. In the absence of intensity non-uniformities, all such voxels would have the same intensity in *e.g.* the in-phase image I_2. The intensity variations could then be estimated by examining voxels which were located inside the body and which had high f_r values. Approximately 30—80 such voxels are selected in each slice. Finding the required number of voxels is rarely a problem, even in slim subjects. Since the spatial intensity variation was assumed to be gradual, a full non-uniformity map could be obtained by interpolation of the intensity of those voxels using normalized convolution [11]. Finally, the water and fat images were corrected by multiplication by the inverse of the intensity non-uniformity map, see Fig 1.

2.4. Morphon registration and segmentation

The Morphon is a non-rigid registration method [10]. It registers a prototype image to a target image by iteratively deforming the prototype. The method is initiated on a coarse resolution scale and then proceeds to finer scales. On each scale a number of iterations are performed, each consisting of the following steps: deformation field estimation, deformation field accumulation, deformation field regularization and prototype deformation. Similar to other registration methods, the morphon can also be used for atlas based segmentation. This is done by associating each voxel of the prototype image with a label and, after the registration is complete, deforming the labels according to the result-

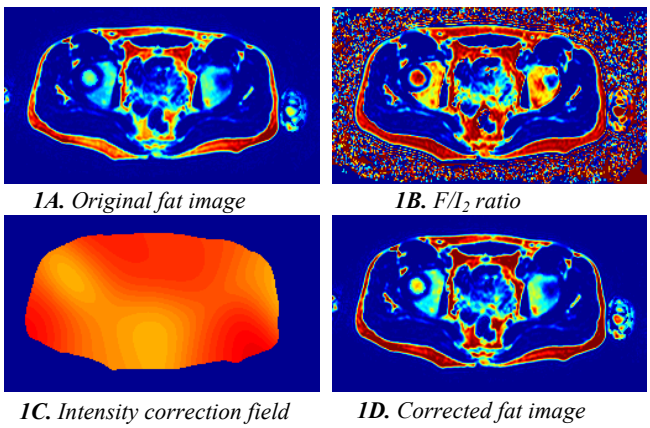

1A. *Original fat image* ***1B.*** *F/I_2 ratio*

1C. *Intensity correction field* ***1D.*** *Corrected fat image*

Fig 1. *Fat, F/I_2, intensity correction field and the corrected fat image obtained during the intensity correction.*

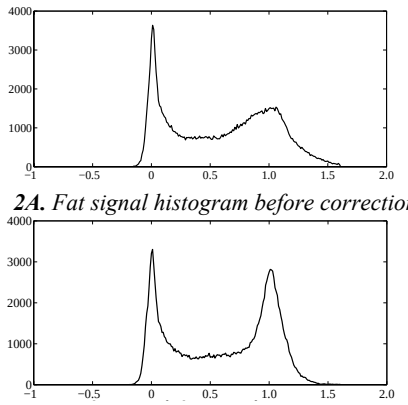

2A. *Fat signal histogram before correction*

2B. *Fat signal histogram after correction*

Fig 2. *Fat signal intensity histograms extracted from the subcutaneous mask before and after intensity correction. Note the significant reduction of the fat peak line width.*

ing deformation field.

The deformation estimate is calculated by maximization of the similarity between the prototype and the target. The similarity measure can be based on e.g. image intensity or local phase information. The latter has the main advantage of being invariant to intensity variations between images. Here we use a phase based approach. A set of directional quadrature filters were applied to the prototype and target data. The local phase difference between the prototype and target filter response in each direction was proportional to the local displacement estimate in the same direction. A least square minimization function was then applied to calculate a single deformation field from the collection of displacement estimates. The calculated deformation fields were accumulated over the iterations and the accumulated deformation field was then regularized using normalized convolution. At the end of each iteration the original prototype was deformed according to the accumulated deformation field after regularization. For more details see e.g. [10].

3. Abdominal registration

In this application, the morphon was used to segment the abdominal adipose tissue into three different types: subcutaneous, visceral and internal non-visceral. This was done by registering a manually segmented prototype to the target image of interest. Registration of an abdominal prototype to a fat image in the abdominal region can be difficult due to the high variability in fat accumulation between different subjects. A significant advantage of the phase sensitive Dixon reconstruction was therefore that separate fat and water images were obtained, yielding additional valuable information. As the water image contains structures with less variability than adipose tissue structures, it was a preferable choice over the fat image for registration intents. However, the water image also contained troublesome areas with high variability. Normalized convolution with a certainty mask decreased the influence of these regions and improved the registration.

To make the process of finding the internal and visceral masks more robust, the registration was divided into two steps. The first step registers a binary prototype to a binary mask of the internal region in the target image. The mask is calculated using local thresholding. This registration was applied on a coarse scale to provide a good initial estimate of the global deformation. When the first step was finished, the resulting deformation field was applied on the second prototype, created from the water image, before proceeding to the finer resolution scales.

An additional certainty mask, covering the muscle and bone structures in the abdominal region, was created to reduce the effects of uncertain regions on the registration result. Finally, masks of the visceral and non-visceral regions were defined for the prototype image. These were used in the segmentation step to label the different compartments of the target image.

Before the registration was launched, the target image was subjected to initial pre-processing steps to create binary masks of the body and of the internal region for the initial registration step. The arms and background of the target image could efficiently be removed from the rest of the body using local thresholding. A local minimum can be expected between the body and arms, and this was used for segmentation of the body. The largest connected component leaves a body mask that is further processed by morphological operations to produce a dense mask.

After the registration had been performed, the calculated deformation field was applied to the labels associated with the prototype image. Hence, the fat in the target image was labeled as *visceral* and *internal non-visceral* parts. Any adipose tissue not associated

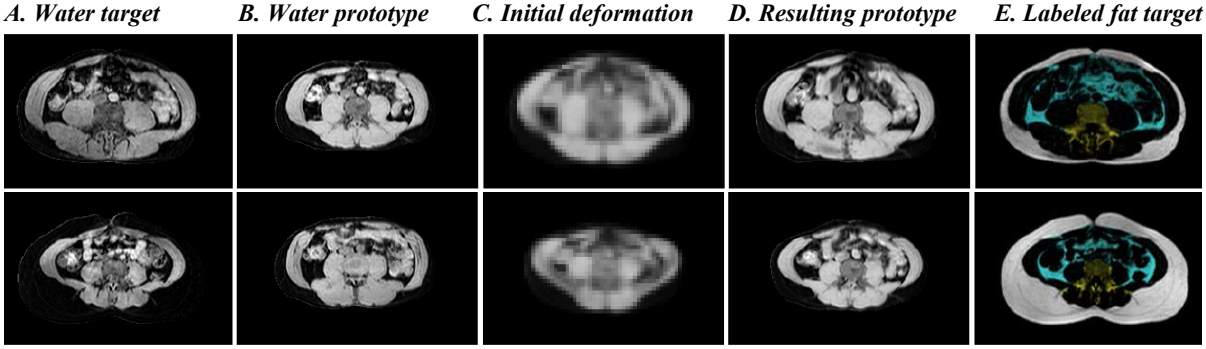

Fig 3. *The different steps of the registration process in two subjects. In A and B the water image of the target and the prototype is shown. In C the resulting prototype after the initial deformation of the binary masks is shown. The final result of the deformation of the prototype is given in D. In E the different labeled fat compartments is shown in the target fat image. Cyan colour corresponds to visceral fat, yellow to internal non-visceral fat and white to subcutaneous fat.*

with any of these labels belongs to the *subcutaneous fat*. Since Dixon imaging provides separate water and fat images, no segmentation was required to distinguish between these types of tissue. The sole purpose of the segmentation process was to divide the adipose tissue into different types.

4. Method validation

The intensity normalization was evaluated on 49 examinations. A fat signal intensity histogram was extracted before and after correction in the two upper image stacks from the body mask. The full width half maximum (FWHM) estimated from the upper half maximum signal intensity and the fat peak signal intensity was estimated

9 randomly selected subjects (5 males and 4 females) were selected for comparison of the performance of the automatic morphon based segmentation against manual segmentation before and after the intervention period. Three different slices well separated within the abdomen were segmented into subcutaneous, visceral and internal non-visceral compartments by an experienced radiologist. A confusion matrix was then calculated for each examination comparing the integrated fat volumes obtained using the automatic method to the manual results regarding the manual results as true volumes.

5. Results

The morphon registration method was used to register and segment subcutaneous, visceral and internal non-visceral compartments. The typical process and final results are illustrated by Fig. 3 where examples in two subjects at different slice levels are shown.

The histograms extracted from the fat image under the body mask had a detectable fat peak in 35 of 49 histograms prior to the intensity normalization. The histograms without identifiable fat peaks occurred in lean subjects only. After intensity normalization 46 histograms showed a detectable fat peak. The estimated FWHM (extracted from examinations where a detectable fat peak was observed both before and after intensity normalization) decreased from 57 ± 14% (measured relative estimated fat peak intensity) to 17 ± 4%, see Fig 2. The standard deviation of the estimated fat peak signal intensity decreased from 9.5% to 1.3% of the mean fat peak signal.

The confusion matrix comparing the morphon based segmentation against manual segmentation is shown in Table 1, displaying mean values and standard deviation of the integrated fat content within the volumes.

	Man. subc.	*Man. visc.*	*Man. intern.*
Auto. subc.	**96.0 ± 1.5 %**	**0.1 ± 0.1 %**	**3.9 ± 1.5 %**
Auto. visc.	**0.3 ± 0.5 %**	**87.7 ± 5.3 %**	**11.9 ± 5.0 %**
Auto. intern.	**1.3 ± 1.2 %**	**2.1 ± 2.7 %**	**96.6 ± 2.9 %**

Table 1. *Confusion matrix comparing automatic and manual segmentation. Each number is the fraction of the manually classified fat given by the automatic method (mean± SD).*

6. Discussion

The methods presented here provide excellent segmentation results also when the target image differs substantially from the prototype. An important aspect of the method is that the registration of the prototype to the target volume is performed exclusively on the water images, which leads to elimination of registration errors from the subcutaneous fat. All algorithms operate in 3D which greatly improves the results of the preprocessing steps as well as the segmentation.

The validation results show a very strong reduction of signal intensity variations within and between different subjects. This means that the method provides very accurate integration of the fat content within the different compartments, avoiding the partial volume effects associated with methods based on summation of voxels in segmented strongly T1 weighted images.

7. References

[1] C. Li et al. Increasing Trends in Waist Circumference and Abdominal Obesity among U.S. Adults. *Obesity*, vol. 15, pp. 216–224, 2007.

[2] M.H. Fishbein, et al. Relationship of hepatic steatosis to adipose tissue distribution in pediatric nonalcoholic fatty liver disease. *J Pediatr Gastroenterol Nutr.*, vol. 42(1), pp. 83–88, 2006.

[3] J. Rydell, et al. Phase sensitive reconstruction for water/fat separation in MR imaging using inverse gradient. In *Int. Con. on Med. Im. Comp. Comp-Ass Interv (MICCAI'07)*, Brisbane, Australia, Oct. 2007.

[4] L.F. Donnelly, et al. Using a phantom to compare MR techniques for determining the ratio of intraabdominal to subcutaneous adipose tissue. *Am. J Roentg*, vol. 180(4), pp. 993–998, 2003.

[5] W.T. Dixon. Simple proton spectroscopic imaging. *Radiology*, vol. 153(1), pp. 189–194, 1984.

[6] J. Ma. Breath-hold water and fat imaging using a dual-echo two-point dixon technique with an efficient and robust phase-correction algorithm. *Magn. Reson. Med.*, vol. 52, no. 2, pp. 415–419, 2004.

[7] S. M.-H. Song et al. Phase unwrapping of MR phase images using Poisson equation. *IEEE Trans. Im. Proc.*, vol. 4, no. 5, pp. 667– 676, May 1995.

[8] E.M. Akkerman and M. Maas. A region-growing algorithm to simultaneously remove dephasing influences and separate fat and water in two-point dixon imaging. In *Proc. ISMRM Ann Meet.*, Nice, France, 1995, ISMRM, p.649.

[9] S. Kechagias, et al. Fast food based hyper-alimentation can induce rapid and profound elevation of serum alanine aminotransferase in healthy subjects. *GUT*, Epub 14 Feb. 2008.

[10] H. Knutsson and M. Andersson. Morphons: Segmentation using Elastic Canvas and Paint on Priors. In *IEEE Int. Conf. Im. Proc. (ICIP'05)*, Genova, Italy, September 2005.

[11] H. Knutsson and C-F. Westin. Normalized and differential convolution: Methods for interpolation and filtering of incomplete and uncertain data. In *Proc. of IEEE Comp. Soc. Conf. Comp. Vis. Pat. Recog.*, June 1993, pp. 515–523.

[12] Rydell J et al. Three Dimensional Phase Sensitive Reconstruction for Water/Fat Separation in MR Imaging using Inverse Gradient. In Proc. of the Int. Soc. Magn. Reson. Med. (ISMRM 2008). Toronto, Canada.